Internet of Things 23 (2023) 100873

Contents lists available at ScienceDirect

Internet of Things

journal homepage: www.elsevier.com/locate/iot

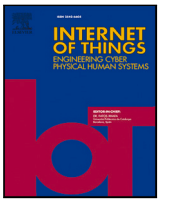

Research article

IoT enabled vehicle recognition system using inkjet-printed windshield tag and 5G cloud network☆,☆☆

Lubna [a], Naveed Mufti [b], Sadiq Ullah [b], Abubakar Sharif [c], Muhammad Waqas Nawaz [a], Ahmed Alkhayyat [d], Muhammad Ali Imran [a], Qammer H. Abbasi [a,*]

[a] James Watt School of Engineering, University of Glasgow, UK
[b] Department of Telecommunication Engineering, UET, Mardan, Pakistan
[c] Department of Electrical Engineering, Government College University, Faisalabad, Pakistan
[d] Department of Computer Technical Engineering, The Islamic University, Najaf, Iraq

ARTICLE INFO

Keywords:
IoT
Vehicle recognition system
UHF RFID
Windshield tag
5G cloud
Internet of Things
Radio frequency identification
ANPR

ABSTRACT

An IoT-enabled vehicle recognition system is developed and tested in this work, besides the tag antenna design and prototype for the vehicle windshield. Firstly, a flexible, surface-tolerant, low-profile, and low-cost passive UHF-RFID windshield tag inlay is designed. The tag is prototyped as wet-inlay with silver conductive-ink inkjet printed antenna on Polyethylene-Terephthalate layer, bonded with Higgs-EC IC. The dimension of the antenna is $0.25 \times 0.05\lambda_0$. The overall inlay structure is around $0.27 \times 0.06\lambda_0$. The antenna is designed at ETSI band, with a return loss of −14 dB at 900 MHz and a read range of 13.3 m and 8 m over lower and upper bands, respectively. The antenna demonstrates an omnidirectional radiation pattern and a maximum gain of 1.92 dBi. The developed prototype is tested in both indoor and outdoor environments. Secondly, the data is sent over the IoT cloud where decision-making is made for authorization. The reader data is transmitted over MQTT broker, via the Scotland 5G network to the MongoDB database using Python module Pymongo. The algorithm for vehicle recognition is written and verified by testing the dummy registered tags for access authorization, with a 100% recognition accuracy. We achieved higher read ranges, surface tolerance, and low profile features, comparatively. The overall system shows optimally great results.

1. Introduction

The Internet of Things (IoT) is creating potentially countless possibilities by enabling devices/objects to connect and share data. Integrating physical equipment or assets to IoT improves services, productivity, and efficiency, therefore, helping industries to mainstream their goals in terms of cost reductions, improved operational efficiency, enhanced productivity, lesser business risk, and improved compliance. IoT is an integral part of Industry 4.0 and has significant applications in industrial automation and monitoring service production systems. Its main objective is facilitating greater performances in multiple disciplines like liquid level monitoring [1], smart factories minimizing costs and errors [2], and for applications beyond Industry 4.0 [3]. A comprehensive

☆ This document is the results of the research project for which grants were provided by the Higher Education Commission of Pakistan.
☆☆ The supervision, research, and prototype facilities were provided by the Communication Sensing and Imaging Group (CSI), James Watt School of Engineering, University of Glasgow, UK.
* Corresponding author.
E-mail address: Qammer.abbasi@glasgow.ac.uk (Q.H. Abbasi).

https://doi.org/10.1016/j.iot.2023.100873
Received 12 June 2023; Received in revised form 3 July 2023; Accepted 5 July 2023
Available online 8 July 2023

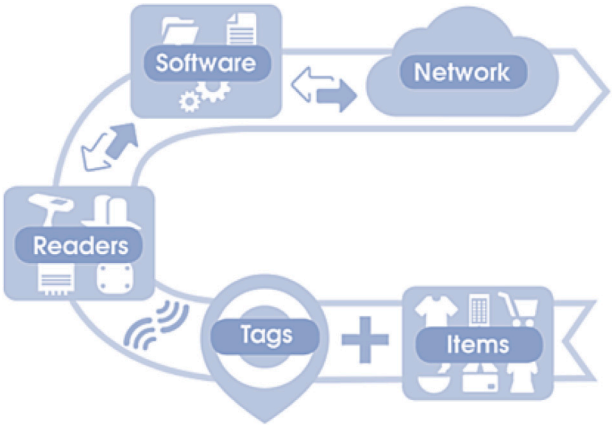

Fig. 1. Schematic of RFID bridging the physical world with IoT network.

literature for IoT is provided in [4], discussing its infrastructures-frameworks, emerging enabling technologies, and potential applications in Industry 4.0 and beyond.

Radio Frequency Identification (RFID) is one of the key-enabling technology and the main perspective fueling its use in IoT-enabled tracking and recognition applications. RFID bridges the physical and digital world for IoT applications. Some of these 'things' may also have IP addresses and integrated computers, but many will be smaller, cheaper devices with no power supply or network access. As the IoT gains popularity, most networked things will be wirelessly connected through low-cost passive RFID technology. While RFID enables the fundamental network-ability of everyday items, RAIN RFID[1] links the dots for a comprehensive network system [5]. Fig. 1 shows a schematic of RFID bridging the physical world with an IoT network.

Automatic Number Plate Recognition (ANPR) using Ultra High Frequency (UHF) RFID technology is one of the majorly deployed on-road IoT applications and is the main focus of this work. In 1991, the first RFID-based electronic toll systems were used in the United States [6]. RFID applications in access controls, intelligent parking systems, toll collection, transportation, and other areas have received significant research attention [7–12]. RFID may be used to address other problems, such as improving the performance of traffic law enforcement systems that employ cameras to recognize vehicle registration numbers. Speed cameras, which are an essential component of most identification systems, are expensive and rely on good visual conditions to identify registration plates. UHF-RFID is a viable alternative for vehicle identification systems, under EPCglobal Class1 Gen2 management — RFID standards & regulations [13]. The cost of radio identification equipment is significantly lower, and it is more weather-resistant. In addition, UHF RFID can scan tags from a sufficient distance to make radio identification possible. If the tag has its own power source and can initiate communication with the reader, the system is active; otherwise, it is passive. Passive RFID typically has a shorter reading range since the signal must travel double the distance from the reader to the tag and back, resulting in considerable signal attenuation. However, these tags are more inexpensive than the active tags and do not require internal power [14]. In spite of huge progress in the field there is still not a single standard of spectrum regulations followed worldwide. Each region has defined its own regulated frequency band for RFID operations. The regulated bandwidth for RFID operations in various regions is provided in [15].

In this study, we designed a flexible, surface-tolerant, low-cost passive UHF RFID inkjet printed tag antenna that is low-profile and delivers longer read ranges than currently available windscreen tags. The novelty of this work is best described in context to the antenna design itself, which is briefly described in Sections 3 and 4. We designed and fabricated a tag for use in IoT-enabled ANPR applications. For efficient electromagnetic radiation to/from the tag, the geometry of the inlay is engineered using the simulation tools, in such a way that the antenna impedance is matched with that of the chip impedance while achieving a miniaturized structure (with a comparatively smaller radar cross-section, yet better read range). This tag achieves a higher read range while maintaining miniaturized dimensions and comparatively lower costs as compared to the other tags available in the literature and commercially, as shown in Table 1. The related work is presented in detail in Section 2. To validate its use in an IoT-based Vehicle Recognition System, the designed tag inlay is tested experimentally in both indoor and outdoor environments and the results are shared in respective sections.

The block diagram of the proposed system is shown in Fig. 2. A complete IoT-enabled vehicle authorization system is developed and tested in this work, besides the tag antenna design and prototype for the vehicle windshield. The tag antenna has a dimension of $0.25 \times 0.05\lambda_0$ (where λ_0 is the wavelength calculated at the central frequency), which is designed using the electromagnetic simulation tool CST Microwave Studio. The read range measurements in European Telecommunications Standards Institute (ETSI/EU — 865–868 MHz & 915–921 MHz) band is up to 13.3 m. The tag results for multi surfaces show that this tag is surface-tolerant and can be utilized in multiple other IoT applications employing objects with these surfaces. The tests were conducted in both

[1] The RAIN RFID Alliance is affiliated with AIM Global (Association for Automatic Identification and Mobility), the global authority on automatic identification, data collection, and mobile networking.

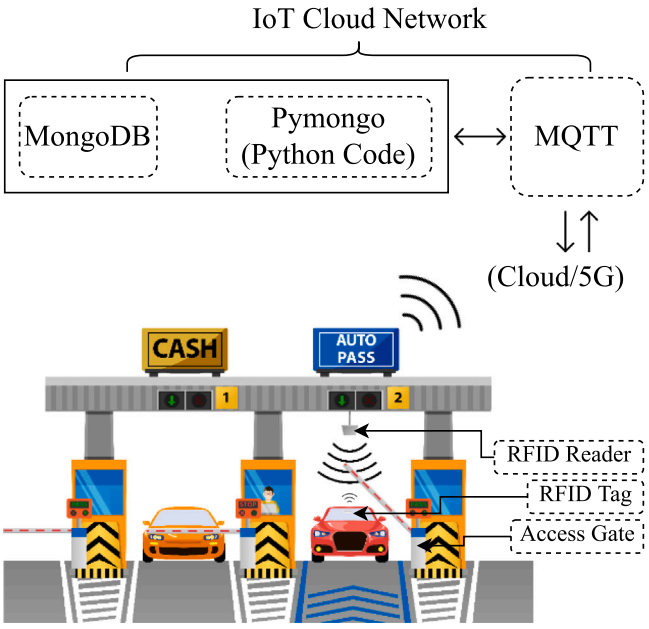

Fig. 2. Block diagram of proposed IoT-enabled vehicle recognition system.

Table 1
Comparison of measurement results of our proposed work with related work.

From	Model	Electrical specifications					Mechanical specifications		
		Op. freq. (MHz)	Read range	Intl. standard.	IC type	Memory	Antenna size	Tag form factor	Attach. method
[16]	ALN-9654	840–960	~6 m	EPC global Class 1 Gen 2 (ISO 18000-6C)	Higgs 3	EPC 96 bits, User 512 bits, TID 64 bits	93 × 19 mm	Dry inlay/ Wet inlay	Adhesive
	ALN-9954	840–960	NA	EPC global Class 1 Gen2 (ISO 18000-6C)	Higgs 9	EPC 96/496 Bits, User Up to 688 Bits, TID 32 Bits	93 × 19 mm	Dry inlay/ Wet inlay	Adhesive
[17]	Windshield Label Anti-Void 7628	860–960	~6 m	EPC global Class 1 Gen2 (ISO 18000-6C)	Impinj Monza R6P	128 bits EPC, 96 bits EPC, 64 bits user	94 × 24 mm	Wet inlay	Plastic Mix
[18]	Onsite Printable Windshield Tag	840–960	~12.8 m	EPC global ISO 18000-63 compliant, Gen2v2	Impinj Monza R6	EPC 96 bits	111.12 × 73.02 mm	Wet inlay	EZ-Peel, Removable adhesive
[19]	Rearview Mirror Hang Tag	840–960	~5.5 m	EPC global Class 1 Gen2 (ISO 18000-6C)	Higgs 3 Higgs 4	EPC 96 bits, User 512 bits, TID 64 bits	Small: 88.9 × 88.9 mm Large: 88.9 × 165.1 mm	Dry inlay	Hanging
[20]	R6 DogBon	840–960	~6.1 m	EPC Class 1 Gen2, ISO 18000-6C	Impinj Monza R6	EPC 96 bits	94 × 24 mm	Wet inlay	RA-2, Permanent UV acrylic hot melt adh.
[21]	LicensePlate Tag	FCC/US 902–928	~20 m	EPC Class 1 Gen2, ISO 18000-6C	Higgs 4	EPC 96 bits, User 512 bits, TID 64 bits	440 × 140 mm	Aluminium Plate	Screws Mount
[22]	MeanderLine Tag	FCC/US 902–928	~11.3 m	EPC Class 1 Gen2, ISO 18000-6C	XRAG2	432 bit Memory	75 × 44 mm	Rogers Substrate	Mount
Proposed	Windshield Tag Inlay	ETSI/EU 865–868 FCC/US 902–928	~13.3 m ~8–10 m	EPC global Class 1 Gen2 (V 1.2.0) ISO/IEC 18000-6C	HiggsEC	512 Bits Total, 96&128 bits, EPC User 128 bits, TID 48 bits	82 × 18 mm	Wet inlay	Adhesive

indoor and outdoor scenarios. In the lab, Tagformance® Pro Unit (Industry standard in RFID measurements) is used for testing the tag performance, whereas, Impinj R-700 RAIN RFID reader is used for testing in an outdoor environment for vehicle windshield. The reader sends information to one or more tags by modulating an RF (Radio Frequency) carrier using a Pulse Interval Encoding (PIE) format. Tags receive their operating energy from this same modulated RF carrier. Tags communicate information by backscatter modulation. Both the modulation and encoding schemes needs to be in accordance with the Global Standards (GS1) for the EPCglobal Gen2 and ISO/IEC 18000-6C protocols defined for communication. It is the manufacturer's responsibility to comply with these while fabricating the tags.

The data sharing in this system occurs through the use of an IoT network protocol called Message Queuing Telemetry Transport (MQTT). It utilizes the MongoDB database and employs the Python module Pymongo to connect to the IoT cloud. The reader data is sent over the Scotland "5G network" to the database by means of an MQTT broker.

Table 2
List of nomenclature.

Symbol	Description	Symbol	Description
V_{ant}	Voltage at tag antenna terminal	G_{read}	Gain of reader antenna
Z_{chip}	Chip Impedance	G_{ant}	Gain of tag antenna
Z_{ant}	Antenna Impedance	λ	Wavelength
R_{chip}	Chip resistance	d	Distance between tag and reader
R_{ant}	Antenna resistance	r	Read range
X_{chip}	Chip reactance	λ	Wavelength
X_{ant}	Antenna reactance	Ω	Ohm (Unit of resistance)
P_{chip}	Power absorbed by the chip	pF	Pico Farad (Unit of capacitance)
P_{ant}	Power received by tag antenna	Q	Quality Factor (a measure of a reactance's purity)
τ	Transmission Co-efficient	MH_z	Mega Hertz (Unit of frequency)
P_{th}	Min threshold power	ϵ_r	Dielectric constant
P_{read}	Power transmitted by reader antenna	dBm	Power expressed in decibels

The algorithm for vehicle recognition is written and verified by testing the dummy registered tags for access authorization. The output dashboard displays results for successful access authorization for registered vehicles and vice versa. The results show that the algorithm is highly efficient and can be deployed in access authorization systems for on-road IoT applications using our proposed tags, ensuring longer distance read range detection. The complete IoT system is tested successfully with a 100% accuracy of decision-making using our python script. Its experimental setups and results are shared in respective sections.

The rest of the paper is arranged as follows. The related work is provided in 2. A description of relevant concepts for antenna design theory and utilized equations is described in 3 to help put the results in context. The design of RFID inlay and electromagnetic simulation results are presented in 4. The fabrication process and prototype measurements are presented in 5, wherein RFID Tagformance® test setup for lab and associated results are discussed in 5.1, while the outdoor test setup and results in 5.2. The test results for the deployment of an RFID system, integrating it with IoT through the MQTT network protocol, are provided in 6. Finally, the work is concluded in 7. Please note, the terms IC, microchip, and chip are used interchangeably.

2. Related work

Many RFID antennas are proposed in the literature for vehicle identification applications. [23] put forward a novel idea by exploiting the characteristic modes and using the vehicle registration number plate as a radiator. The existing number plate is optimized by creating slots and introducing a feed structure into the 440 × 140 mm number plate. The read range claimed here is about 20 m using a Higgs-4 chip at 915 MHz. However, integrating this into the existing infrastructure seems infeasible and impractical, since this would require upgrading the registration numbers with slots and feed structures, for every single vehicle, that too when a low-cost RFID tag solution is available for similar purposes. In order to address the localization of on-road vehicles, [22] presented a meander-line UHF RFID tag antenna which achieved a read range of 11.7 m and has dimensions of 75 × 44 mm. However, this tag is designed over a limited frequency band of 918 MHz center frequency. The substrate used is Rogers R04450B which is not flexible and neither low-cost. Furthermore, the results shared for read range are merely theoretical and no calculation criteria are presented for it. The tag is not fabricated to measure the actual read ranges, which in most cases are always different from the theoretical ones. Similarly, [21] presented a windshield tag antenna for vehicle identification systems, with a feed point meander-line geometry on a laminated-glass substrate, for vehicle identification and tracking. It has a 15 m read range but a complex fabrication process with higher costs as compared to the existing flexible low-cost RFID tags in the market. Now comparing the available inlays with our proposed design; in [16,17], wide-band windscreen tags are presented for vehicle recognition systems. The size of this tag is larger while the read range achieved is only 6 m which is lower than the proposed tag in our work. The inlay presented in [18] has a relatively good read range of 12.8 m but the size is quite large. The proposed RFID tag is compared with other state-of-the-art designs presented in the literature for on-road applications, regarding its performance and measurement results as listed in Table 1. The proposed tag has been prototyped and tested over various surfaces, and measurements have been recorded. The proposed tag is tested in both indoor and outdoor environments to measure read ranges and tolerance over different surfaces. The main application focus of this work is to design a robust tag antenna, develop it into a prototype, and its IoT integration into the system, to ensure its use in on-road applications such as contactless payments at toll plazas, access control, traffic analysis, tracking vehicle historical movements, parking management systems, free-flow traffic and, as a result, eliminating congestion and optimizing the entire process to be smooth and efficient.

The following sections validate the use of our proposed tag inlay in IoT-enabled on-road applications. A list of nomenclature is provided in Table 2, to assist readers in interpreting the content accurately.

3. Antenna design theory

RFID tags are primarily made up of an antenna and a microchip, which have complex impedance as illustrated in Fig. 3. Chips are normally bonded to the antenna terminals, and the reader's interrogating field powers them through the voltage (V_{ant}) generated at the antenna terminals. Thus, in order to improve the read range of an RFID system where the tag is driven by electromagnetic induction, the impedance of the tag's antenna should be optimally matched with that of the chip [24].

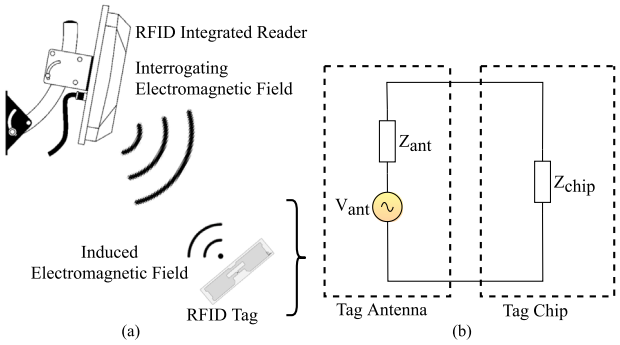

Fig. 3. Schematic of RFID system and an equivalent circuit of RFID inlay.

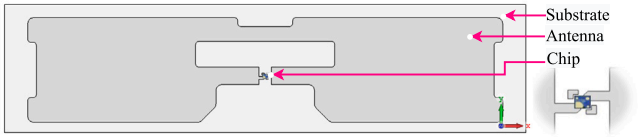

Fig. 4. General structure of passive UHF RFID tag inlay, consists of metallic track (antenna), substrate, and a microchip.

A general structure of passive UHF RFID inlay is shown in Fig. 4. An RFID Inlay is just the RFID chip (IC), tag antenna, and substrate, typically on a film face. If the substrate has adhesive it is termed wet-inlay, otherwise, it is called dry-inlay.

From [25,26], and the equivalent lumped circuit illustrated in Fig. 3b, the chip impedance Z_{chip} and antenna impedance Z_{ant}, which are frequency dependent, can be expressed as follows:

$$Z_{chip} = R_{chip} + jX_{chip} \tag{1}$$

$$Z_{ant} = R_{ant} + jX_{ant} \tag{2}$$

where, R_{chip}&R_{ant} are the chip and antenna resistance, and X_{chip}&X_{ant} are the chip and antenna reactance, respectively. $Vant$ is an open-circuit RF voltage generated by the reader electromagnetic field at the tag antenna terminals. The impedance of the chip, Z_{chip}, is dependent on the power absorbed by the chip, P_{chip}, and usually has energy-sapping effects. The impedance of the current commercial chip generally presents a large capacitive reactance and a small resistance. Such a high-Q chip impedance makes it difficult to match the antenna design, which also limits the impedance bandwidth of the antenna. The reflection coefficient due to mismatch must be less than a certain level. The power absorbed by the tag chip P_{chip} can be expressed in terms of the maximum available power from the antenna P_{ant} and the power transmission coefficient τ, as follows:

$$P_{chip} = P_{ant}\tau \tag{3}$$

Maximum antenna power P_{ant} is attained when $Z_{chip} = Z_{ant}$. The power transmission coefficient τ specifies the impedance match between the IC and the antenna, and is given as follows:

$$\tau = \frac{4 * R_{chip}R_{ant}}{Z_{chip} + Z_{ant}} \tag{4}$$

As τ approaches unity, the tag chip and antenna impedance match improve. While $\tau = 1$ shows an ideal complex conjugate match between the IC and antenna impedance. Therefore, for a given chip-and-tag antenna configuration $\tau = 1$ would be ideal, where $Z_{chip} = Z_{ant}$. Moreover, the antenna used in the RFID system is typically adjusted to match the minimum threshold power P_{th} required for activating the RFID chip.

While impedance matching is a crucial aspect of RFID tag design, the read range of the tag design, along with the reader and reader antenna, holds greater significance, as depicted in Fig. 3a. The read range of a combined tag and reader system is defined by two factors: (i) The maximum range at which the tag receives the minimum P_{th} signal necessary to activate the chip and initiate signal backscattering, and, (ii) The maximum range at which the reader can detect and pick up these returned signals.

The maximum range at which a reader can detect a strong return signal is significantly larger than the maximum range where a tag can receive P_{th} to switch on and scatter back. To ensure this, the reader system's power settings or antenna can be adjusted accordingly. So, for this work, the read range will be realized as the farthest point from which the tag can get the minimum P_{th} it needs to activate and scatter back the signal.

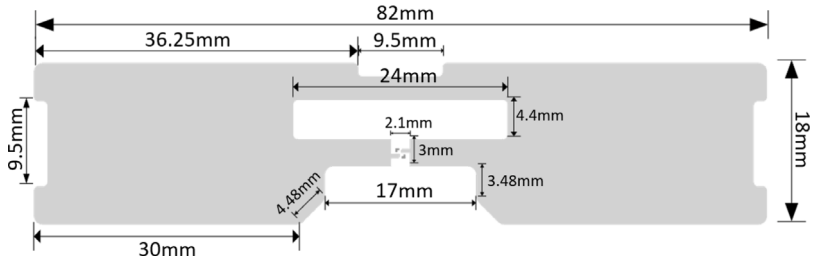

Fig. 5. Simulation model: Geometry of proposed windshield RFID tag antenna with dimensions.

The free-space tag antenna power P_{ant} is calculated using the $Friis$ free-space equation, where:

$$P_{ant} = P_{read} G_{ant} G_{read} (\frac{\lambda}{4\pi d})^2 \tag{5}$$

where P_{read} and G_{read} is the reader-transmitted power and antenna gain respectively. G_{ant} is the tag antenna gain, λ denotes the wavelength, and d is the distance between the tag and reader.

Substituting in (3) and the read range r is the distance at which the tag receives the minimum P_{th}, gives the read range as follows:

$$r = \frac{\lambda}{4\pi} \sqrt{\frac{P_{read} G_{ant} G_{read} \tau}{P_{th}}} \tag{6}$$

The peak read range r throughout a frequency range is known as the tag's resonance and it correlates with the maximum power transmission coefficient τ. Therefore, to achieve the largest read range, it is necessary to optimize the tag antenna for maximum power transmission coefficient τ and then calculate r based on (6) along with the reader system.

The RFID system's read range (forward and reverse link) is dependent on four system parameters: (i) Reader radiated power, (ii) Reader sensitivity, (iii) Tag back-scatter signal intensity, and (iv) Tag sensitivity. The forward link describes reader-tag communication where the reader transmits the signal (radiated power) and the tag receives it (tag sensitivity). The reverse link describes tag-to-reader communication which involves scattering back the signal to the reader (tag back-scatter intensity) and the reader detecting this signal (reader sensitivity).

4. Design of RFID inlay and electromagnetic simulations

There are many ways to achieve a perfect impedance match between chip and tag antenna, e.g., increase parasitic loops, use dual radiators to generate adjacent resonant frequencies to increase bandwidth, use inductive/capacitive coupling to feed, adding coplanar lines, etc, to the design structure. The proposed design uses the method of slots on the radiation patch. By adding a T-slot on the center of the radiator and slots on the sides of the antenna, the original surface current path is cut off consequently which makes the current flow through the side of the slot. Furthermore, the current path becomes longer. In other words, it is equivalent to introducing cascaded inductance into the antenna equivalent circuit, which makes the antenna input impedance present larger inductive reactance. In this case, it can achieve a good match with the chip which has larger capacitive reactance. By changing the size of the T-slot and the slot on the short side of the antenna, the input impedance of the antenna can be adjusted, which is beneficial for the matching between the antenna and chip with different impedance. A schematic of the proposed low-profile RFID inlay with dimensions is shown in Fig. 5.

The overall dimension of the antenna is $0.25 \times 0.05\lambda_0$ (82×18 mm). λ_0 is the free space wavelength of the center frequency. The frequency band of operation for this tag is 865–868 MHz covering the intended ETSI/EU RFID band in accordance with the allowed range for the application for mentioned demographics. However, this antenna works well on the global frequency range of operation 860–960 MHz. The antenna simulation model is designed at center frequency of 900 MHz.

The antenna is specifically designed to work with the Higgs-EC IC from Alien Technology. This IC has an input impedance that can be represented as a 2500 Ω resistor and a 0.95 pF capacitor connected in parallel. Additionally, the IC has a reading sensitivity of −20 dBm, which corresponds to the minimum power required to wake up the IC. At a frequency of 900 MHz, the input impedance of the chip is approximately 14–j186 Ω.

The electrical specifications of the IC are shown in Table 3. Using equations from Section 3, we calculated the impedance of the IC using electrical characteristics provided from manufacturer datasheet [27].

For resistor–capacitor parallel circuit:

$$Q = R_p \times \omega C_p \tag{7}$$

From Table 3, the equivalent parallel resistance R_p is 2500 Ω and parallel capacitance C_p is 0.85 pF + 0.1 pF parasitic capacitance, So Q at 900 MHz can be calculated. According to circuit theory, the real part of the chip impedance R_{chip} is equal to:

$$R_{chip} = \frac{R_p}{1 + Q^2} \tag{8}$$

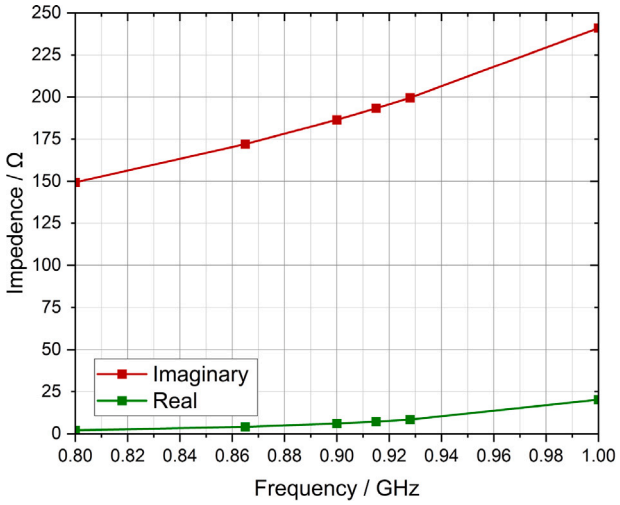

Fig. 6. Complex impedance plot of the simulation model showing resistance (real) and reactance (imaginary) values.

Table 3
Operational characteristics of Higgs IC.

Symbol	Parameter	Min/Max	Units
Operating Conditions			
T_A	Operating Temperature	−50 + 80	°C
f_{in}	Operating Frequency	840 to 960	MH_z
Electrical Characteristics			
$\boldsymbol{S_R}$	Read-Sensitivity	**−20**	**dBm**
S_W	Write-Sensitivity	−14.8	dBm
$\boldsymbol{R_p}$	Resistance (Parallel)	**2500**	**Ω**
$\boldsymbol{C_p}$	Capacitance (Parallel)	**0.85**	**pF**
D_{ret}	Retention of Data	50	Years

In this case, we calculate R_{chip} = 13.9 Ω. The imaginary part of the chip impedance is $1/(\omega Cp)$ and is equal to −186 Ω. Utilizing (1), Z_{chip} = 14–j186 Ω, which is close to the conjugate impedance of the tag antenna. The impedance plot is shown in Fig. 6. To achieve an impedance match we adjusted the length L, of the main T-slot. Fig. 7 shows the reflection coefficient (S parameter-S11), with a 14 dB return loss of the tag antenna at 900 MHz, which shows that the performance is relatively good. The far-field radiation patterns show an omnidirectional pattern with a max antenna gain of 1.92 dBi. Its 3D and polar plots are shown in Fig. 8. The radiation efficiency at 900 MHz is 96%, which shows good performance.

We achieved a higher read range and low profile compared to the commercially available windshield tags in the market from various fabricants. A comparison of the proposed windshield tag inlay with others is presented in Table 1.

5. Prototype/fabrication and measurements

The dielectric constant (ε_r) for different Polyethylene-Terephthalate (PET) substrates varies from 2.4 to 3.6. The antenna is printed over a flexible PET substrate with ε_r 2.8 and a thickness of 0.05 mm. The antenna is printed with silver nano-particle conductive ink using inkjet printing technology.

Hot melt adhesives are later on added to the prototype. The chip is bonded to the antenna which holds the object's essential data/information as required for the application. Higgs-EC EPC-Global-Gen2 IC from AlienTechnology is used, which boasts faster writing, increased sensitivity of −22.5 dBm, and a faster read rate. The "EC" in the chip's name stands for Error Correcting. Errors do occasionally happen in RFID systems during bit coding and transmission. If a tag is damaged or hacked, the bit could possibly flip, which changes a number or many numbers in the transmission. The reader will then relay the wrong information. This new EC chip corrects these errors in case they ever happen while reading/writing. The horizontal die length of the IC is 0.49 mm, the vertical die length is 0.479 mm, and the die thickness of 0.15 ± 0.01mm. Pad placement and dimensions of the IC are shown in Fig. 9. All dimensions are in thousandths of a millimeter and +/−10.

5.1. RFID tagformance® test: Setup and results of prototype

To verify the simulation results and the read ranges of the designed RFID inlay, we took two experiment setups for the prototype testing. The lab measurements are done by Tagformance® Pro device and the Tag Designer Suite (TDS) software while the outdoor

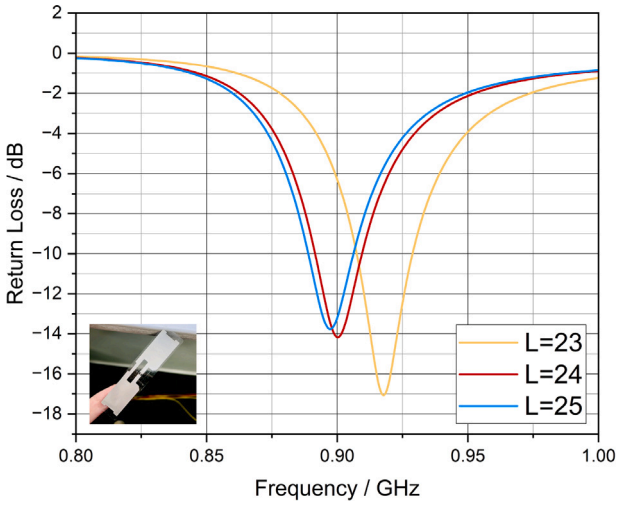

Fig. 7. Return Loss: S11 — Reflection coefficient of the proposed tag inlay.

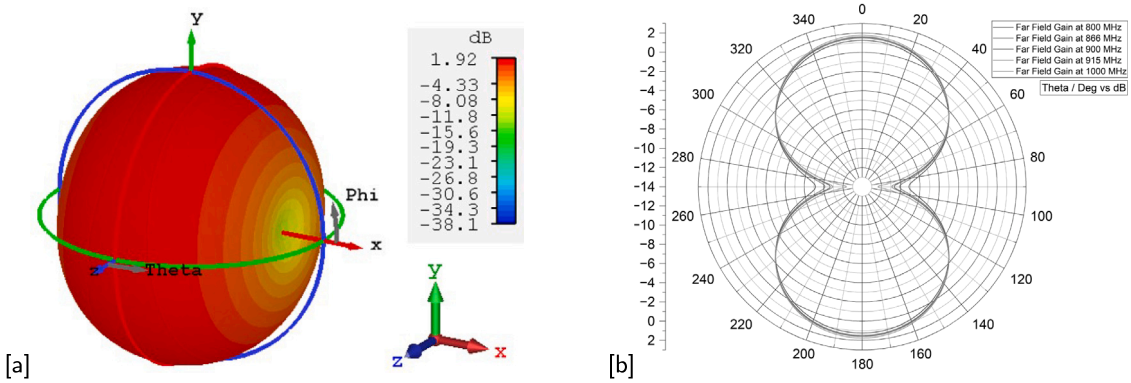

Fig. 8. Radiation pattern of simulation model (a) 3D view of far-field gain at λ_0, (b) polar plot of far-field gains at 800–1000 MHz.

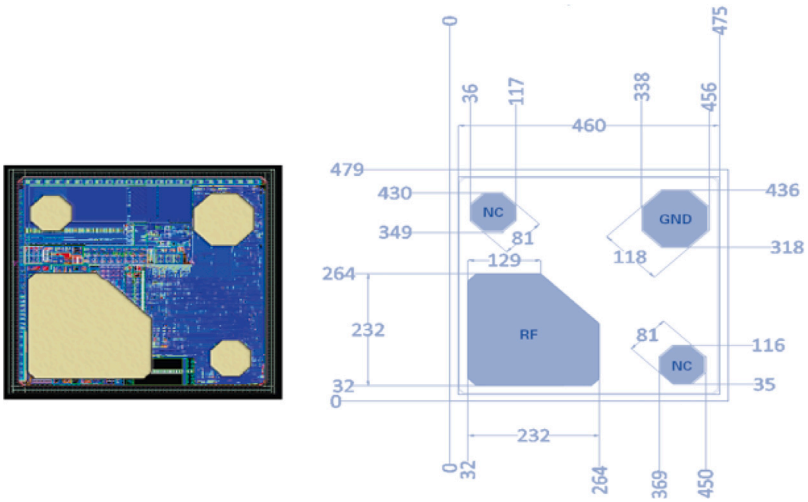

Fig. 9. Pad placement and dimensions of Higgs EC IC.

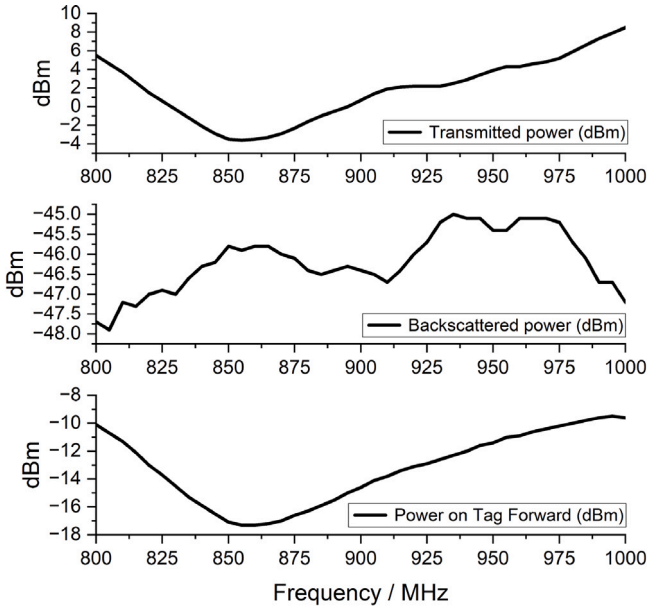

Fig. 10. Analyzed power on tag forward, and backscatter signal at 800–1000 MHz with multiple transmit-power levels.

test is performed using an Impinj R-700 reader. Tagformance® is a complete industrial measurement solution for evaluating the performance of RFID tags. The RFID system's read range (forward and reverse link) is dependent on four system parameters: (i) Reader radiated power, (ii) Reader sensitivity, (iii) Tag back-scatter signal intensity, and (iv) Tag sensitivity. In the read range test, tag sensitivity is evaluated over a frequency range of 800 MHz to 1000 MHz, and the power on tag forward, and backscatter signal is analyzed at each frequency with multiple transmit-power levels as shown in Fig. 10. The global standard regulatory limit for UHF RFID applications is typically 2 Watts ERP (Effective Radiated Power), in many countries, including the UK. Compliance with these allowed ERP ranges is essential for adhering to regulatory requirements and ensuring the safe and efficient operation of RFID systems. Due to the regional restrictions, the Tagformance Pro device used in our research was limited to a maximum ERP of 2 W. This limitation prevented us from directly adjusting the power settings to increase the read ranges during our testing. We adhered to standard power settings for our experiments.

The experimental setup is shown in Fig. 11. The recorded read range for the proposed windshield tag and industrial windshield tag from Alien Technology ALN-G at ETSI band is shown in Fig. 12. The proposed tag has a read range of around 12 m at 866 MHz, the central frequency of ETSI band, whereas the ALN-G tag perform well with a read range of 7.8 m in the same band. The proposed tag was also tested on various surfaces like plastic, cardboard, book, wood, polystyrene, fabric, PVC, etc. The read range results of the multi surfaces test are shown in Fig. 13. The read range can be observed for both ETSI and FCC/US bands. In the ETSI band, with a read range of above 7.5–11.5 m, most surfaces perform well since the tag is optimized at the central frequency in the ETSI band. For the FCC band, the same tag has a read range of 5–7 m for various surfaces without any tag optimization. The proposed tag is also tested in an indoor environment, using the Impinj R-700 Reader, in the university corridor and the measured read range recorded is 13.3 m. These results indicate that the tag can be read from a long distance of 13 m in indoor environments. Also, the tag is surface tolerant and can be utilized for multiple other IoT applications in supply chain or retail setups.

5.2. RFID system outdoor test: Setup and results of prototype

In the outdoor experiment, the RFID tag is applied 4 inches down from the top, at the middle of the vehicle windshield, and the read range is measured using Impinj R-700 Reader with a 6 dBi circular antenna. The outdoor setup is shown in Fig. 14, which is carried out at the main parking avenue of the University of Glasgow, UK. The reader was able to detect and read the tags at an 8–10 m distance. The results show good efficiency for the proposed tag as compared to the other tags in Table 1, in terms of read ranges and size compactness which is just 82 × 18 mm. The proposed tag can be utilized for on-road applications including control access systems, e-toll collection points, parking management systems, distance estimation, etc.

6. RFID system deployment test: IoT integration using MQTT network protocol

The chip on the RFID tag stores the necessary information about any object. In this case, we tested the proposed tag for vehicle authorization systems. The chip contains the vehicle registration number which is linked to the database containing all necessary information about the vehicle including vehicle ownership, registration date, and current balance for auto toll deductions

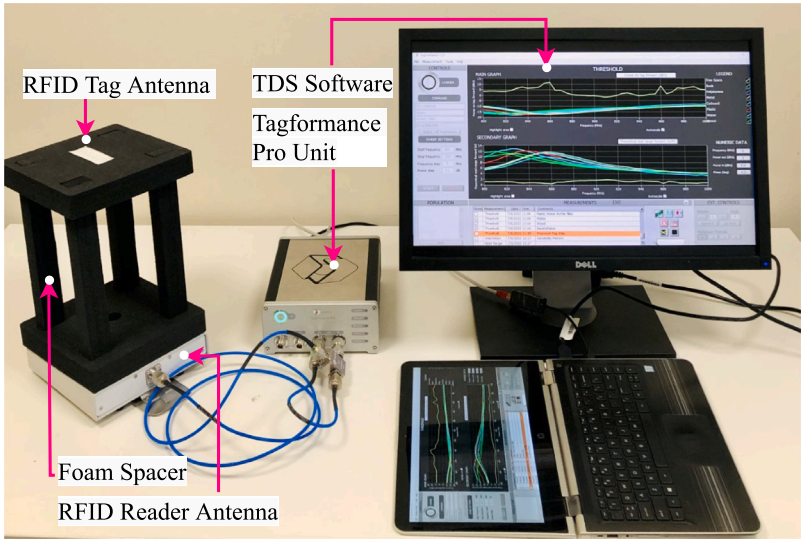

Fig. 11. Testing setup: Tagformance Pro device and antenna under test.

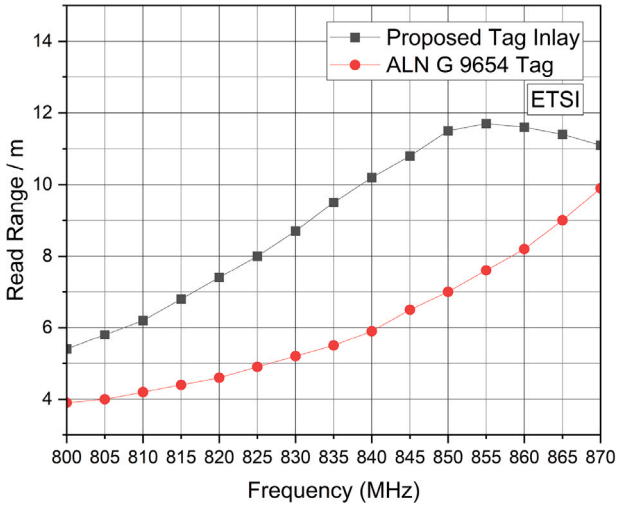

Fig. 12. Read range measurement of proposed tag and ALN-G tag at ETSI band using Tagformance Pro device.

or authorization access. The recorded information for each vehicle can be communicated to the control server from the readers' database, using cloud solutions for further processing according to the application being used. The network topology used in our IoT-enabled vehicle recognition system is a cloud-based architecture. The IMPINJ R700 RAIN RFID reader has a simple IoT device interface that easily connects IoT applications to configure, control, and consume data, with native support for MQTT protocol. It operates on top of the TCP/IP protocol, making it efficient in terms of network utilization and data transmission.

In our proposed system for authorization access and electronic toll collection, when the RFID reader reads a vehicle tag, its data is transmitted over MQTT broker via the Scotland 5G network to the MongoDB database via Python module Pymongo. The python script is then listening to the same MQTT broker and will act on each message that is sent. Firstly it will load the data to a dictionary and extract the car's ID number from the EPC value sent. From here it will check if that ID is known to the system by searching it in the database, and if so, does that account have a high enough balance to pass. If the account has a high enough balance it will reduce this by the given price, update the database with the new amount, then approve that user. If the account is unknown to the system, or its balance is lower than the price to pass through, then the user will be denied access and the relevant reason will be shown. During this process, the timestamp is saved for that account and will not be charged multiple times. After the decision is made the authorization is either granted for the registered vehicles or denied otherwise. The decision-making algorithms and output display the possible scenarios provided. To test our algorithm, 10 tags are assigned dummy registration numbers as WT-01, WT-02, to WT-10. These registration numbers are associated with the vehicle and contain information about the vehicle owner and the

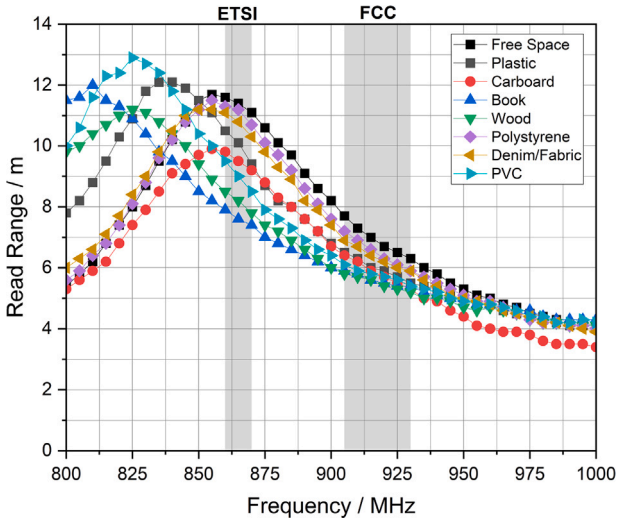

Fig. 13. Read range measurements on different surfaces.

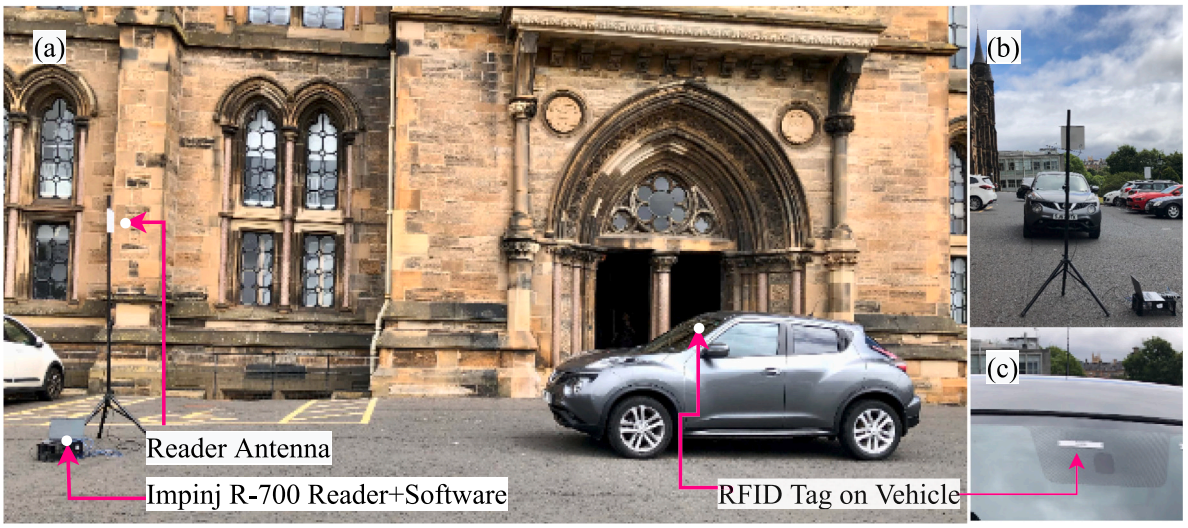

Fig. 14. Experimental setup in outdoor, (a) side view, (b) front view, (c) proposed tag pasted on a vehicle windshield.

current balance for the e-toll pass. These tags are granted authorization access. We designed 3 different scenarios, (i) the vehicle is registered and has enough balance to pass the toll, (ii) the vehicle is registered and has insufficient balance to pass the toll (iii) the vehicle is not registered irrespective of the balance. The flow chart of the process is given in Fig. 15. We tested these tags randomly and all of these tags were provided access successfully. We tried with unregistered tags and the access was denied which shows the system is working efficiently with 100% accuracy for IoT-enabled on-road applications ensuring longer read range detection for smooth traffic flow.

Generally, when a reader is exposed to multiple RFID tags, it can lead to interference and tag collisions. The overlapping signals from different tags can cause data corruption or loss, impacting system performance. Anti-collision techniques are employed to mitigate these issues, allowing the reader to communicate with multiple tags in an organized manner. The level of interference and effectiveness of anti-collision techniques depend on factors such as tag density, proximity, reader capabilities, and the employed anti-collision algorithms. Moreover, the ability of a reader to handle multiple tags simultaneously varies depending on its design and specifications. Some readers are equipped with advanced anti-collision algorithms and signal processing capabilities to manage and handle a higher number of tags efficiently. These readers can effectively mitigate interference and handle multiple tag responses.

Our future work plan is to utilize Long Range Radio-Wide Area Network (LoRa-WAN) technology for IoT applications. The LoRa protocol and LoRaWAN gateway are not yet prioritized because of the scope and practicability of our project. Therefore, for this use case, we took advantage of cloud-based solutions over 5G network. The global expansion of 5G networks is anticipated to lead

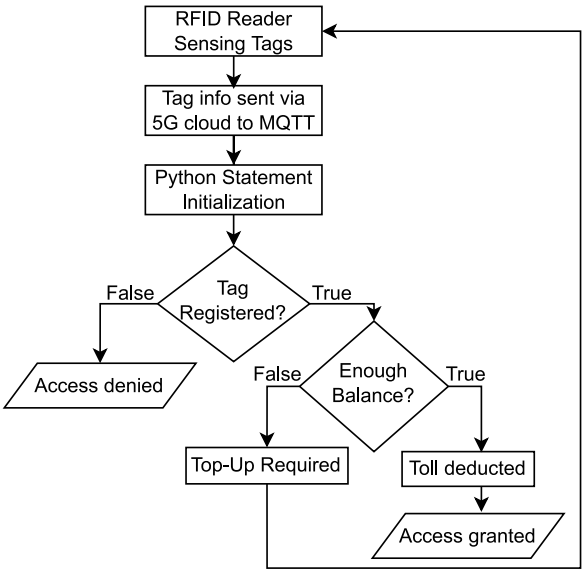

Fig. 15. Flow chart of decision-making algorithm for vehicle recognition system.

to a rise in the use of IoT technology and applications. It is recognized, however, that 5G alone is insufficient for many IoT devices to communicate various sorts of data in real-time. These limitations encourage the development of 6G technologies that can offer more network capacity, reduced latency, and quicker data transfer than 5G networks. [28], presents a thorough survey on current 6G research trends and how they relate to IoT whereas [29] discusses the present state-of-the-art in 5G IoT research, important enabling technologies, and major research trends and problems in 5G IoT. Being a 5G's successor, it is speculated that 6G will not be implemented by 2030 as it is currently at the research and foundation stage. Researchers are working towards the advancements of various factors of 6G, which will enable future applications more secure and transparent with the integration of blockchain services and Artificial Intelligence. [30,31] fulfills the crucial role of bringing practitioners and researchers to a technological perspective and security challenges of future 6G communication technology.

7. Conclusion

In this work, a novel RFID tag inlay for IoT applications is designed, developed into a prototype, and then tested for real use-case in indoor/outdoor environments. Voyantic Tagformance® Pro device was used to measure read range, power sensitivity, and back-scattered signal strength. In the lab test, the read range measured is around 12 m, however, in an indoor test using an Impinj R-700 reader in the corridor, the read range measured was 13.3 m. Outdoors, using an Impinj R-700 reader, the read range is 8–10 m, which shows the tag feasibility in e-toll collection systems, access control systems, smart parking, and other on-road IoT application for vehicles. The proposed tag is also tested on various surfaces like plastic, cardboard, book, wood, polystyrene, fabric, PVC, etc, and the results are shared. It shows that this tag is surface tolerant and can be used for multiple applications in asset management besides windshield tagging for on-road applications. After successful testing of the prototype read ranges, IoT integration is done to complete the system. The reader reads/records the data and transmits it over the MQTT broker via the Scotland 5G network to the MongoDB database via the Python module Pymongo. The python script is then listening to the same MQTT broker and acts on each message that is sent for decision-making. The algorithms for vehicle recognition are written and verified by testing in this work. The output displays results for successful access authorization for registered vehicles and vice versa. The results show the algorithm is highly efficient and can be deployed in access authorization systems for on-road IoT applications using our proposed tags ensuring longer read range detection. The complete IoT system is tested successfully with a 100% accuracy of decision-making using python script. Its experimental setups and results are shared in respective sections.

Declaration of competing interest

The authors declare the following financial interests/personal relationships which may be considered as potential competing interests: Lubna reports financial support, administrative support, and travel were provided by Higher Education Commission Pakistan. Lubna reports administrative support, article publishing charges, equipment, drugs, or supplies, statistical analysis, and writing assistance were provided by University of Glasgow James Watt School of Engineering.

Data availability

Data will be made available on request.

References

[1] J. Bhookya, M.V. Kumar, J.R. Kumar, A.S. Rao, Implementation of PID controller for liquid level system using mGWO and integration of IoT application, J. Ind. Inf. Integr. 28 (2022) 100368.
[2] I.H. Khan, M. Javaid, Role of internet of things (IoT) in adoption of industry 4.0, J. Ind. Inf. Integr. (2021) 2150006.
[3] A. Sigov, L. Ratkin, L.A. Ivanov, L.D. Xu, Emerging enabling technologies for industry 4.0 and beyond, Inf. Syst. Front. (2022) 1–11.
[4] F. Liu, C.-W. Tan, E.T. Lim, B. Choi, Traversing knowledge networks: An algorithmic historiography of extant literature on the internet of things (IoT), J. Manag. Anal. 4 (1) (2017) 3–34.
[5] RAIN RFID, What RAIN RFID brings to the internet of things. [Online]. Available: https://rainrfid.org/resources.
[6] J. Landt, The history of RFID, IEEE Potentials 24 (4) (2005) 8–11.
[7] W. Chen, J. Childs, S. Ray, B.S. Lee, T. Xia, RFID technology study for traffic signage inventory management application, IEEE Trans. Intell. Transp. Syst. (2022).
[8] M. Berlin, S. Selvakanmani, T. Umamaheswari, K. Jausmin, S. Babu, Alert message based automated toll collection and payment violation management system using smart road side units, Mater. Today: Proc. (2021).
[9] W.C. Tan, M.S. Sidhu, Review of RFID and IoT integration in supply chain management, Oper. Res. Perspect. (2022) 100229.
[10] G. Casella, B. Bigliardi, E. Bottani, The evolution of RFID technology in the logistics field: A review, Procedia Comput. Sci. 200 (2022) 1582–1592.
[11] J. Dutta, R. Mathew, An overview of sensors in intelligent transportation systems and electric vehicles, AI Enabled IoT Electr. Connect. Transp. (2022) 61–73.
[12] J.R. Garcia Oya, R. Martin Clemente, E. Hidalgo Fort, R. González Carvajal, F. Munoz Chavero, Passive RFID-based inventory of traffic signs on roads and urban environments, Sensors 18 (7) (2018) 2385.
[13] H. Barthel, Epcglobal–RFID standards & regulations, 2005, Paris, France.
[14] D. Dobkin, The RF in RFID: Passive UHF RFID in Practice (p. 25), Elsevier Inc, Burlington, MA, 2008, p. 72.
[15] GS1, Overview of UHF frequency allocations (860 to 960 MHz) for RAIN RFID, 2022. [Online]. Available: https://www.gs1.org/docs/epc/uhf_regulations.pdf.
[16] Alien Technology, Alien "G" Inlay, ALN-9654 / ALN-9954. [Online]. Available: https://www.alientechnology.com/products/tags/g/.
[17] Dipole | RFID, Windshield RFID label. [Online]. Available: https://www.dipolerfid.com/product/windshield-label.
[18] AtlasRFIDstore, Vulcan RFID onsite printable windshield tag. [Online]. Available: https://www.atlasrfidstore.com/vulcan-rfid-onsite-printable-windshield-tag/.
[19] AtlasRFIDstore, Vulcan RFID custom rearview mirror hang tag. [Online]. Available: https://www.atlasrfidstore.com/vulcan-rfid-custom-rearview-mirror-hang-tag/.
[20] AveryDennison, Dogbone UHF RFID tag and inlay. [Online]. Available: https://rfid.averydennison.com/en/home/product-finder/dogbone.html.
[21] N. Crişan, Laminated glass UHF-RFID antenna for automotive applications, Carpathian J. Electron. Comput. Eng. 12 (1) (2019) 13–16.
[22] R. Jouali, M. Aoutoul, H. Ouahmane, Y. Errami, A. Obbadi, A. Haddad, F. El Moukhtafi, A. Had, A new design of rfid tag for vehicles localisation applications, in: 2019 International Conference on Wireless Networks and Mobile Communications, WINCOM, IEEE, 2019, pp. 1–3.
[23] Z. Liang, J. Ouyang, F. Yang, L. Zhou, Design of license plate RFID tag antenna using characteristic mode pattern synthesis, IEEE Trans. Antennas and Propagation 65 (10) (2017) 4964–4970.
[24] M. Yeoman, M. O'neill, Impedance matching of tag antenna to maximize RFID read ranges & design optimization, in: 2014 COMSOL Conference, Cambridge, UK, 2014.
[25] K.S. Rao, P.V. Nikitin, S.F. Lam, Impedance matching concepts in RFID transponder design, in: Fourth IEEE Workshop on Automatic Identification Advanced Technologies, AutoID'05, IEEE, 2005, pp. 39–42.
[26] A. Zahid, N. Mufti, S. Ullah, M.W. Nawaz, A. Sharif, M.A. Imran, Q.H. Abbasi, et al., IoT-enabled vacant parking slot detection system using inkjet-printed RFID tags, IEEE Sens. J. 23 (7) (2023) 7828–7835.
[27] Alien Technology, Higgs-EC, high sensitivity RFID IC with enhanced data quality. [Online]. Available: https://www.alientechnology.com/products/ic/higgs-ec/.
[28] J.H. Kim, 6G and internet of things: A survey, J. Manag. Anal. 8 (2) (2021) 316–332.
[29] S. Li, L. Da Xu, S. Zhao, 5G internet of things: A survey, J. Ind. Inf. Integr. 10 (2018) 1–9.
[30] Y. Lu, X. Ning, A vision of 6G–5G's successor, J. Manag. Anal. 7 (3) (2020) 301–320.
[31] Y. Lu, Security in 6G: The prospects and the relevant technologies, J. Ind. Inf. Integr. 5 (03) (2020) 271–289.